

Constraining X-ray Binary Jet Models via Reflection

Sera Markoff¹ and Michael A. Nowak

*Massachusetts Institute of Technology, Center for Space Research, Rm. NE80-6035,
Cambridge, MA 02139*

sera,mnowak@space.mit.edu

ABSTRACT

Although thermal disk emission is suppressed or absent in the hard state of X-ray binaries, the presence of a cold, thin disk can be inferred from signatures of reprocessing in the $\sim 2 - 50$ keV band. The strength of this signature is dependent on the source spectrum and flux impinging on the disk surface, and is thus very sensitive to the system geometry. The general weakness of this feature in the hard state has been attributed to either a truncation of the thin disk, large ionization, or beaming of the corona region away from the disk with $\beta \sim 0.3$. This latter velocity is comparable to jet nozzle velocities, so we explore whether a jet can account for the observed reflection fractions. It has been suggested that jets may contribute to the high-energy spectra of X-ray binaries, via either synchrotron from around $100 - 1000 r_g$ along the jet axis or from inverse Compton (synchrotron self-Compton and/or external Compton) from near the base. Here we calculate the reflection fraction from jet models wherein either synchrotron or Compton processes dominate the emission. Using as a guide a data set for GX 339-4, where the reflection fraction previously has been estimated as $\sim 10\%$, we study the results for a jet model. We find that the synchrotron case gives $< 2\%$ reflection, while a model with predominantly synchrotron self-Compton in the base gives $\sim 10 - 18\%$. This shows for the first time that an X-ray binary jet is capable of significant reflection fractions, and that extreme values of the reflection may be used as a way of discerning the dominant contributions to the X-ray spectrum.

Subject headings: radiation mechanisms: non-thermal – accretion, accretion disks – black hole physics – X-rays: binaries

¹NSF Astronomy & Astrophysics Postdoctoral Fellow

1. Introduction

X-ray binaries (XRBs) have been observed in several distinct states, which are characterized by the relative strength of their soft and hard X-ray emission components, as well as by their variability properties (see, e.g., McClintock & Remillard 2003). In the “standard” models (see Reynolds & Nowak 2003, and references therein) the soft component is well-explained with thermal emission from a standard thin disk (Shakura & Sunyaev 1973), while the hard power-law component is generally attributed to inverse Compton (IC) scattering processes. The various models currently in existence often have quite different seed photons and system geometries, yet predict similar results for the broad continuum emission (see Nowak et al. 2002; Markoff et al. 2003). In order to discern between the models, therefore, one has to look at finer details which are dependent upon specific elements of the geometry.

In the hard state, the power-law component dominates the thermal disk emission over most of the X-ray range. The presence of a cold, thin disk can still be inferred via detection of a soft component in the $\approx 0.3\text{--}1$ keV band, and via spectral components in the $\approx 2\text{--}50$ keV band suggesting that a fraction of the hard X-rays is reprocessed or reflected from an optically thick surface. The reflection component is characterized by a flattening of the power-law above ~ 10 keV (e.g., Pounds et al. 1990; George & Fabian 1991), as well as by spectral features such as an Fe $K\alpha$ fluorescent line and an Fe edge (see Reynolds & Nowak 2003, for a review). The strength of these components is directly related to the spectrum and flux hitting the disk, and is therefore sensitive to assumptions about the system geometry. For example, in models where the hard X-rays are due to IC in a hot coronal plasma completely “sandwiching” the disk, the reflection is easily too high for typical X-ray binary spectra (and the self-consistently derived coronal temperatures are too low; e.g., Stern et al. 1995; Dove et al. 1997a). Thus modifications have been proposed, such as a recessed thin disk (Dove et al. 1997b; Poutanen et al. 1997), beaming away from the disk (Reynolds & Fabian 1997; Beloborodov 1999), or large amounts of ionization of the disk (Ross et al. 1999; Nayakshin & Dove 2001; Done & Nayakshin 2001).

In addition to the standard corona models, Markoff et al. (2001) proposed that the entire broadband spectrum of hard state XRBs could instead result from synchrotron emission at the beginning of an acceleration region. While controversial, this model succeeds at explaining the tight correlation of radio and X-ray emission seen in several sources (e.g., GX 339–4, Corbel et al. 2000, 2003; Markoff et al. 2003), which, in fact, may be a universal correlation in XRB hard states (Gallo et al. 2003). It is also the first model to provide a link between the inferred presence of a hot, magnetized electron plasma near the inner regions of the central engine to the hot, magnetized plasma that we know exists via imaged radio jets (e.g., Stirling et al. 2001). A shortcoming of these models, however, is that they have not yet

attempted to explain detailed X-ray spectral features such as reflection and iron lines. In this Letter we calculate the expected reflection fraction from several jet models with parameters that provide good descriptions of broad band features (e.g., overall luminosity, flat radio spectrum, X-ray spectral slope and cutoff) for ‘typical’ XRB data sets, such as those shown here for the Galactic source GX 339–4. We then discuss the ensuing constraints on jet models.

2. Model Background

The amount of X-rays from a jet falling on an element of the disk depends upon the distance between the jet emission zone and disk element, the angle between the jet bulk flow and the line-of-sight to the disk, and the bulk velocity, β_j , of the jet at that zone. A moderately relativistic flow is not necessarily prohibitive, and in fact the resulting aberration has been invoked as a solution to reduce the reflection fraction in hard state sources. Beloborodov (1999) originally proposed this scenario for Cyg X-1, and found that they could explain the observed reflection fraction if a dynamic corona is beamed perpendicularly away from the disk with $\beta \sim 0.3$. Malzac et al. (2001) used a more sophisticated approach to find that the correlations between reflection fraction and spectral index can be explained by varying the bulk flow velocity from $\beta \sim 0.3 - 0.7$. These bulk velocities are typical for weak jets; therefore, a careful treatment of reflection from jet emission may shed light on how models of dynamic coronae can be unified with models of the jet base.

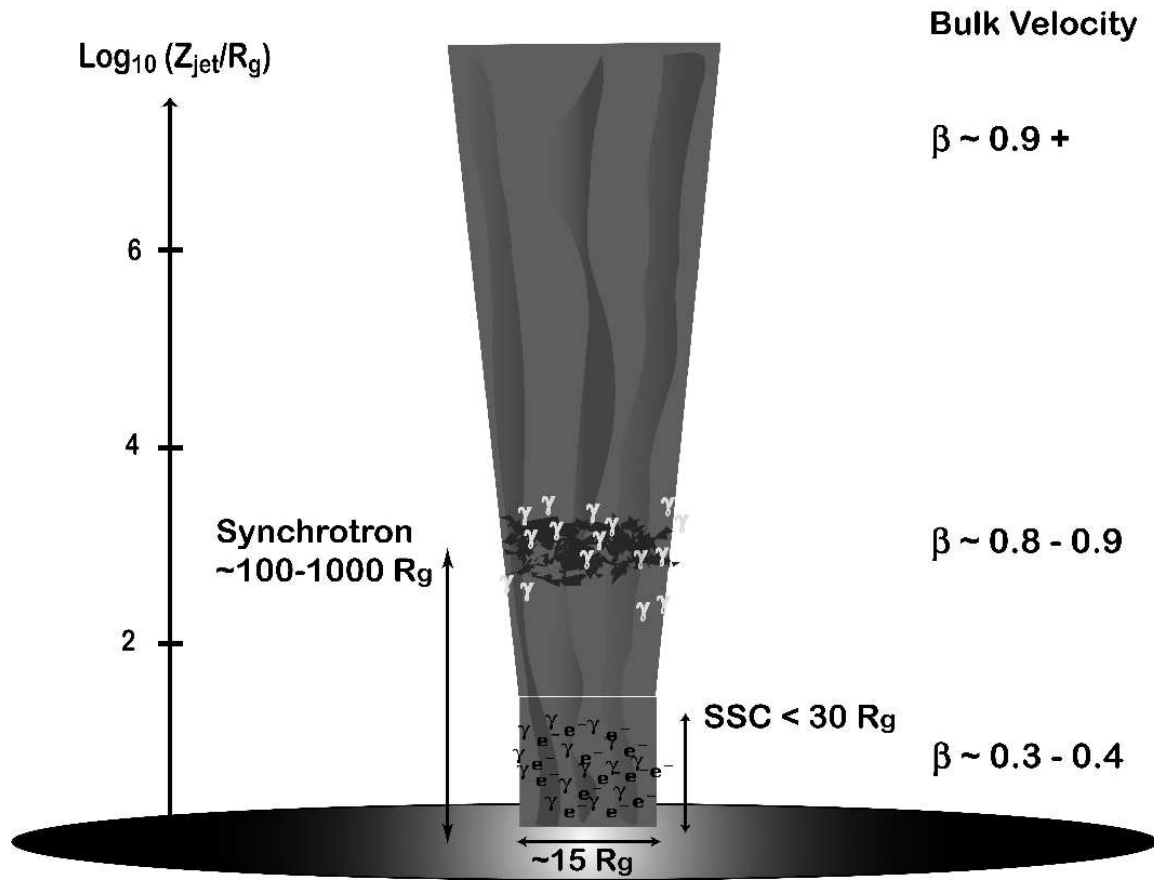


Fig. 1.— Schematic of jet models.

Following Beloborodov (1999), the “reflection fraction” of a relativistically beamed corona can be defined as

$$R(\mu) \equiv \left\langle \frac{dP}{d\Omega} \right\rangle / \frac{dP(\mu)}{d\Omega} \quad , \quad (1)$$

where $dP/d\Omega$ is the emitted power per unit solid angle, $\mu \equiv \cos\theta$, θ is the angle between the direction of coronal bulk motion and the observer’s line of sight, and the angular average is over the half of the sky subtended by the disk. In the absence of beaming, R would be independent of angle and ≈ 1 , since the disk subtends nearly half the sky as viewed from the dynamic corona. The same would be true for our jet models, as the distance from the jet base to its outer X-ray emission region is substantially smaller than the outer disk radius. Beaming serves to reduce the reflection fraction by enhancing the coronal or jet emission along lines of sight in the direction of motion, while simultaneously reducing the amount of emission towards the disk.

In the specific model considered by Beloborodov (1999), the ratio of these two effects yields a reflection fraction of

$$R = (1 - \beta/2) (1 - \beta\mu)^3 (1 + \beta)^{-2} \quad . \quad (2)$$

Even for $\beta \approx 1$, one expects a reflection fraction of 3% for $\mu = 1/2$. Note that a simple answer is obtained as Beloborodov (1999) considers a photon flux per unit energy $\propto E^{-2}$. The spectrum shape, although not its amplitude, is independent of angle, allowing the definition given above.

For the case of our jet models, the spectrum intercepted by the disk has a similar, but not identical, shape to that of the directly viewed spectrum. This makes a translation into a simple value for ‘reflection fraction’ less straightforward, although one still expects fitted values to yield $R \approx 3\%$ if $\beta \approx 1$. Larger reflection fractions can be achieved by decreasing the jet speed and by increasing the fraction of X-ray emission occurring close to the disk surface, e.g., by Compton emission from the jet base.

In the jet models considered to date, there have been propositions for both synchrotron (Markoff et al. 2001, 2003) and external IC (EIC) (Georganopoulos et al. 2002) contributions to the X-rays. In the former models, the components from synchrotron self-Compton (SSC) and EIC from the disk were calculated self-consistently, but were found to fall below the synchrotron emission for the jet parameters considered. The relative Compton contributions can be raised if the assumed scale for the jet is expanded, resulting in lower densities and thus allowing higher electron temperatures. In the synchrotron dominant models that we have previously studied, we had assumed the radius of the jet base to be on the order of the event horizon, specifically, we set $r_0 \sim 3r_g \equiv 3 GM/c^2$ (Markoff et al. 2003). If, on the other hand, the jet base is contiguous with, or generated in, an extended corona, a larger

scale may be more sensible. With this in mind, we have explored a new range of models with $r_0 \sim 15 - 20r_g$.

The dependence of the calculated spectrum upon the model parameters (jet size scale, jet power, electron temperature, etc.), and the interdependence of the model parameters given the assumptions of a ‘maximal jet’, are complex. Increasing the scale of the jet base allows one to decrease the electron density as well as the magnetic field, for a fixed equipartition relationship. This allows one to consider electron temperatures up to a few times higher than those used in our previous models (to make up for lost synchrotron flux). The higher electron temperatures lead to greater Compton emission relative to synchrotron processes in the X-ray band. It is important to note that, compared to the synchrotron emission, the Compton emission occurs close to the central black hole in a region of lower bulk velocities ($\beta \approx 0.3$). However, the beaming is enough to significantly reduce the amount of reprocessed disk radiation reaching the jet for inverse Compton upscattering. The photon field from the rest frame synchrotron emission in the jet is typically orders of magnitude higher than even the direct disk photon field. Reprocessed disk radiation will be significantly less and thus its feedback on the X-ray spectrum will be negligible. We thus do not include this in the following calculations.

In Fig. 1, we show a schematic of the jet model, indicating the approximate locations of the synchrotron and EIC/SSC emission regions, as well as their bulk velocities. The jet base starts out as a nozzle flow of constant radius moving at the speed of sound, $\beta_s = \sqrt{(\gamma_a - 1)/(\gamma_a + 1)} \sim 0.4$ for our adopted adiabatic index $\gamma_a = 4/3$. In the case of a free jet, which we assume here for simplicity, it accelerates only due to its longitudinal pressure gradient. The velocity profile of the jet, $\beta_j(z)$, is then determined by solving the Euler equation along the jet axis (see Falcke 1996). Ignoring terms of order $\ln \gamma_j \beta_j$, one finds $\gamma_j \beta_j \simeq \sqrt{\beta_s^2 (\gamma_a + 4 \ln(z/z_0))}$, where z_0 is the length of the nozzle. The jet also expands laterally with β_s , and the resultant adiabatic cooling of the particles is taken into account.

Models and scaling arguments based on active galactic nuclei (AGN) jets suggest that the turnover from optically thick to thin jet synchrotron in XRBs occurs in the IR/NIR. Such a turnover is seen explicitly in a 1981 observation of GX 339–4 (Corbel & Fender 2002). For our model, this corresponds to a region at $\sim 100\text{--}1000 r_g$ in the jet, and represents the start of the acceleration zones. In contrast, both SSC and EIC from the disk are strongest at the base of the jet in the nozzle regime.

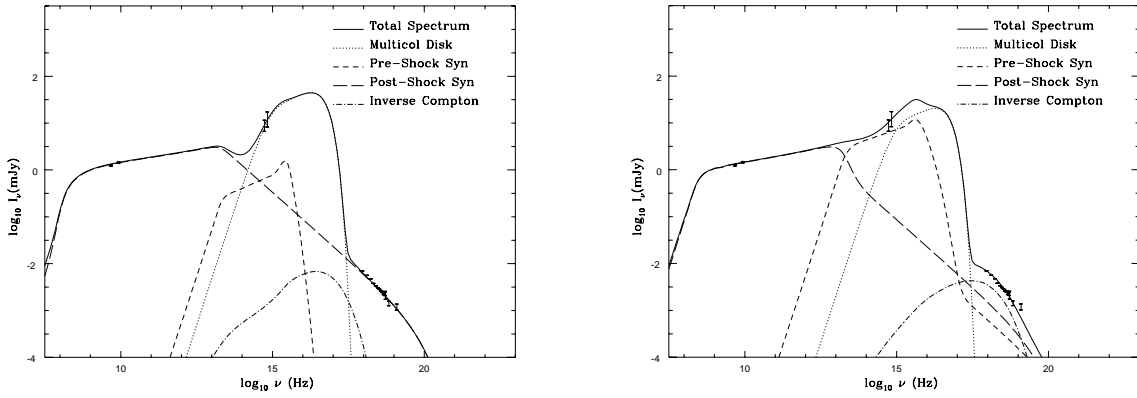


Fig. 2.— Jet model representative fits for multiwavelength GX 339–4 observations from 1999 May 14 (see Nowak, Wilms, & Dove 2002). a) Synchrotron-dominated regime similar to what was presented in Markoff et al. (2003), but with jet nozzle $r_0 = 15 r_g$ and electron temperature $T_e = 7 \times 10^9$ K, with equipartition parameter $k \equiv B^2/8\pi/\int n_e(E_e)dE_e = 3$. Roughly 10% of the particles are accelerated. b) Synchrotron self-Compton dominated regime with jet nozzle $r_0 = 15 r_g$ and electron temperature $T_e = 2 \times 10^{10}$ K, with $k=30$. In this fit, $\lesssim 1\%$ of the particles are accelerated, further suppressing the synchrotron component.

3. Calculation

3.1. Direct Jet Emission

In order to test the amount of reflection expected from both regions in our model, as well as to test the dependence upon the plasma velocity, we have performed four calculations. We have calculated the spectra of both a synchrotron-dominated and an SSC-dominated model, and for each type of model we employ $\beta_s \sim 0.4$, as described above, as well as a slower jet model with $\beta_s \sim 0.3$ (with $\beta_j(z)$ scaled accordingly). In Fig. 2 we show representative plots of a synchrotron- and an SSC-dominated model for one of the simultaneous radio, IR and X-ray data sets used in Markoff et al. (2003). This particular data set is from 1999 May 14 (RXTE observation 40108-02-03-00, labeled “99_3” in Markoff et al. 2003). It represents a source hard state, several months after the return from a prolonged soft state, as the source was fading into quiescence. This particular observation had a reflection fraction of $R \approx 0.1$ when fit by coronal models (the `eqpair` code; Coppi 1999).

The models in Fig. 2 have not been convolved with the raw X-ray data through the detector response matrices. We recently have succeeded in importing the jet continuum model into the `XSPEC` software analysis package¹ (Arnaud 1996), in order to begin addressing the detailed features of the spectrum. For instance, there has been some question as to whether jet models can describe the shape of the spectrum near the ~ 100 keV cut-off region in the hard state. We will focus on this question in detail elsewhere (Markoff & Nowak, in prep.); however, here we include for reference a preliminary figure for the Galactic BHC Cyg X-1 (Fig. 3), which exhibits evidence of a rather steep cut-off. Applying the jet model to the 10 – 200 keV region, we obtain a very good description of the broadband X-ray continuum, including the turnover region. This is a promising start, but we need to consider further details such as line emission and a soft component. We further need to determine how to incorporate the reflection results presented here into a self-consistent, but also time-efficient, fitting procedure.

¹The fit shown below, however, was performed in `ISIS v1.1.7` Houck & Denicola (2000), which incorporates all `XSPEC` models including ‘local models’, and will allow us to more readily include radio and optical data in future fits.

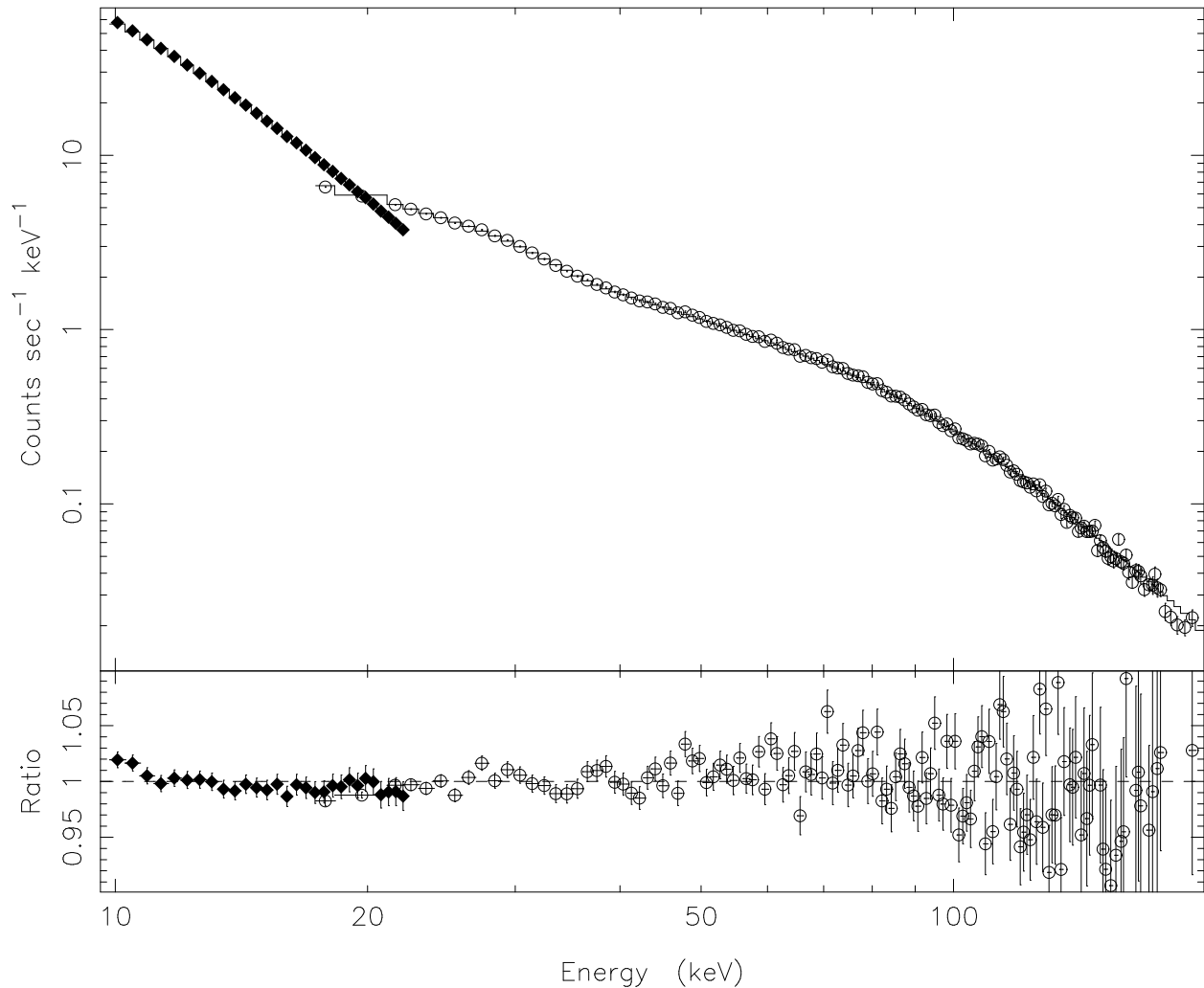


Fig. 3.— Jet model (similar to that shown in Fig. 2b), without reflection components, fit to 10-200 keV spectra from the low/hard state of Cyg X-1. This spectrum has been previously presented by Pottschmidt et al. (2003) (rev. 11 in that paper). These data are from the RXTE instruments PCA (10-22 keV; solid diamonds) and HEXTE (18-200 keV; clear circles), extracted using the `HEASOFT v5.3` tools. Systematic errors of 0.5% have been applied to the PCA data; however, no systematic errors have been applied to HEXTE. The PCA data has been rebinned to have a minimum of 20 counts per bin, while HEXTE has been rebinned to have a minimum signal-to-noise ratio of 8 in each bin. Using `ISIS v. 1.1.7` (Houck & Denicola 2000) to perform the fits, we obtain a reduced $\chi^2 = 1.6$ for 173 degrees of freedom. The quality of this data description, including the excellent fit to the high energy rollover, is comparable to that of coronal Comptonization fits (Pottschmidt et al. 2003).

3.2. Reflected Jet Emission

In order to calculate the reflection spectra of the jet, we divide the jet into ~ 80 logarithmically spaced slices along its axis, from $\sim 3 - 10^8 r_g$. The effect of relativistic beaming is applied to the emission from each jet element, and we calculate the angle-dependent flux intercepted by an annulus of the disk, which is divided into 100 logarithmically spaced annuli between radii of $6 r_g$ to $10^5 r_g$. For a given disk annulus, the total intercepted flux is calculated by integrating the beamed jet emission over the full extent of the jet. We have not considered the effects of gravitational focusing of the emission towards the disk; however, this is likely to be negligible for the synchrotron-dominated jets where the X-ray emission is coming from $\sim 100-1000 r_g$. We are likely, however, to be underestimating the amount of reflection from the SSC-dominated jets where a significant fraction of the emission occurs close to the inner disk.

Our approach is to calculate the emission from each segment of the jet as if it were coming from the center of the segment along the jet axis, which is a reasonable approximation from far away. At its very base, however, the jet radius is larger than the inner radius of the disk. In order to account for this region, we perform a separate calculation of the nozzle emission at the jet base. Using $\mu = -1$ in the beaming factor, we integrate the jet base emission impinging upon the disk out to r_0 . The direct emission from the jet, taking $\mu = 0.77$, is calculated as described by Markoff et al. (2003). We further assume that observer only sees X-ray emission from one side of the jet and disk.

The integrated jet emission hitting each radial bin is then taken and passed through an ionized reflection code (`pexriv`) and then relativistically smeared using a Schwarzschild metric, as appropriate for Keplerian rotation at each radius (see Magdziarz & Zdziarski 1995; Zdziarski et al. 1995; Życki et al. 1997). The specific usage of these widely available codes was adapted from the `eqpair` code, where we have taken advantage of the `eqpair` spline fits of the continuum spectrum before it is passed to the reflection routines (Coppi 1999). For Fig. 4 we have taken a neutral disk with solar abundances, and we adopt $\mu = 0.77$ for the reflected spectrum, as with the direct jet emission.

4. Results and Discussion

As a first step towards judging the magnitude of the reflection fraction, we can calculate $R(\mu)$ as a function of energy by substituting $dP/d\Omega d\nu$ into eq. 1. The synchrotron-dominated cases show the smallest overall reflection. The ratio is only $\approx 1-2\%$ in between energies of 1–100 keV ($\beta_s = 0.3, 0.4$). The ratio peaks at 0.3 keV with value 6% and 8% for $\beta_s = 0.3$

and $\beta_s = 0.4$, respectively. The SSC-dominated jet shows significantly more reflection. For $\beta_s = 0.3$ and $\beta_s = 0.4$, the ratio is $> 10\%$ in between 0.5–23 keV. The former peaks at 18% at 6 keV, while the latter peaks at 17% at 5 keV. Such values of ‘reflection fraction’ are comparable to the observed range for GX 339–4, and in fact are larger than fitted for this particular observation (Nowak et al. 2002).

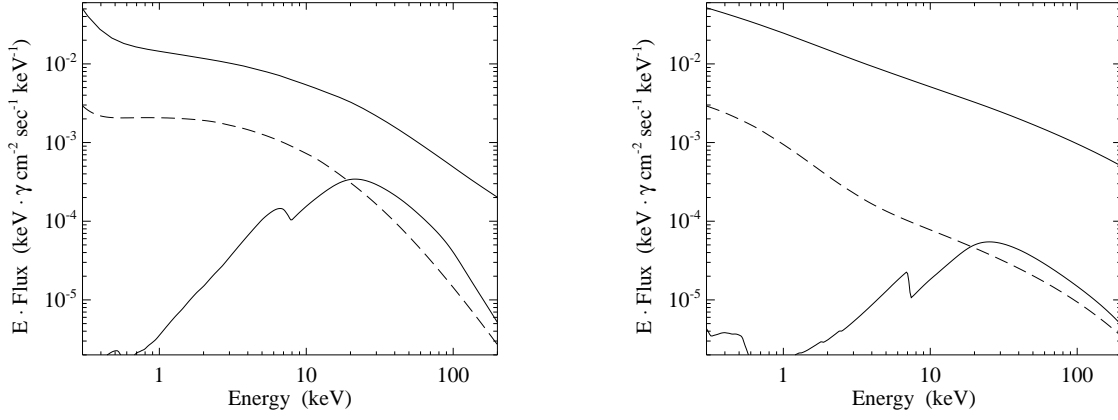


Fig. 4.— Total model spectrum (direct plus reflected - solid line), summed spectrum incident upon the disk (dashed line), and reflected spectrum (lower solid line). *Left*: SSC-dominated jet with $\beta_s = 0.4$. *Right*: Synchrotron-dominated jet with $\beta_s = 0.4$.

As described above, we have also directly calculated the reflection spectrum expected from our models. We show spectra for the SSC-dominated jet and the synchrotron-dominated jet, both with $\beta_s = 0.4$, in Fig. 4. Qualitative differences are immediately apparent. The SSC-dominated jet clearly has an overall brighter reflection spectrum, and effects of relativistic smearing are readily visible. These effects are to be expected given both the lower velocities of the SSC-dominated region ($\beta \sim 0.3$) as well as the fact that this region is closer to the central black hole.

We have chosen a slightly face-on orientation, $\mu = 0.77$, since there has been some suggestion that this is indeed the case for the GX 339–4 system (Wu et al. 2001). Most BHC systems should have a higher inclination, which, given eq. 1, allows for even greater reflection fractions. If we freeze all of our model parameters but instead choose $\mu = 0.5$, reflection fractions, as defined by the ratio of the disk-incident spectrum to the directly viewed spectrum, increase. Over the 1–20 keV interval, this ratio is everywhere $> 26\%$ for the SSC-dominated jet with $\beta_s = 0.3$, and $> 7\%$ for the synchrotron-dominated jet with $\beta_s = 0.4$. The former peaks at 38% at 2 keV and, again, exhibits clear relativistic broadening of the reflection features.

While still preliminary, this is the first time that the reflection of jet emission off an accretion disk has been calculated for an X-ray binary system. These results show that jets are indeed capable of producing the reflection fraction inferred from the X-ray data, providing further support for a connection between the base of the jet and the corona. We have highlighted two extreme cases which might be applicable to different physical situations. Systems that exhibit very low reflection ($\lesssim 5\%$), with sharp (i.e., non-relativistic) features in any reflected spectrum (e.g., XTE J1118+480, Miller et al. 2001), could be synchrotron-dominated, and clearly rule out SSC-dominated jets. Systems with significantly larger reflection fractions ($\gtrsim 15\%$) cannot be synchrotron-dominated, especially if they exhibit features which are unambiguously relativistically smeared. However even in the Compton-dominated regime, as shown in Fig. 2, synchrotron radiation can contribute $\gtrsim 10\%$ of the flux which, as we discuss further below, will greatly effect fits to data with corona plus reflection models.

For intermediate values, or values $\gtrsim 30\%$, other factors need to be considered. For instance, these results assume that the disk is perfectly flat, and that the jet is always perpendicular to the disk. Realistically, disks are expected to flared or warped (e.g., Dubus et al. 1999), and several systems also show evidence for misalignment between the jets and outer disks (Maccarone 2002). Both of these effects will serve to increase the reflection fraction from the jet, particularly for the synchrotron component. Therefore, we treat these numbers as lower limits.

We would like to emphasize, however, that a significant X-ray contribution from jet

synchrotron emission can greatly alter how one even defines ‘reflection fraction’ based upon a presumed single-component, underlying continuum. As shown in Fig. 3, jet radiation alone can provide a good description of the high energy cutoff region. One can readily imagine a model wherein the soft X-ray region is dominated by SSC emission (as in Fig 4b) and/or Comptonization of external (disk) photons, each with a large covering factor of the disk (i.e., essentially unity reflection fraction, for that component alone). The hard X-ray radiation could then be dominated by synchrotron radiation with inherently low reflection fraction. The net spectrum would have an intermediate fitted value of ‘reflection fraction’ that does not have a ‘geometric interpretation’ entirely appropriate for either the soft or hard emission components. If the broad-band X-ray continua of hard state BHC are in fact comprised of such multiple components, as in some of the jet models presented here, then this calls into question current interpretations of ‘reflection fractions’ based upon single component fits.

Of course, in order to determine whether such multiple spectral components are indeed present in the observations, actual fitting of the combined direct plus reflection spectrum needs to be performed. The calculations and models presented here provide vital clues as to how much each process can contribute for this next step. This work has shown that this type of analysis may hold the key to disentangling the emission processes relevant from the accretion inflow and outflow, and place limits on the synchrotron vs. Compton contributions to the hard state spectrum.

We would like to thank Jon Miller for encouraging us to make this calculation, and Jörn Wilms for a careful reading of the manuscript. S.M. is supported by an NSF Astronomy & Astrophysics postdoctoral fellowship, under NSF Award AST-0201597. This work has also been supported by NSF Grant INT-0233441 and NASA Grant NAS8-01129.

REFERENCES

- Arnaud, K. A. 1996, in *Astronomical Data Analysis Software and Systems V*, ed. J. H. Jacoby & J. Barnes No. 101 (San Francisco: ASP), 17
- Beloborodov, A. M. 1999, *ApJ*, 510, L123
- Coppi, P. 1999, *PASP Conference Series*, 161, 375
- Corbel, S. & Fender, R. 2002, *ApJ*, 573, L35
- Corbel, S., Fender, R. P., Tzioumis, A. K., Nowak, M., McIntyre, V., Durouchoux, P., & Sood, R. 2000, *A&A*, 359, 251

- Corbel, S., Nowak, M., Fender, R. P., Tzioumis, A. K., & Markoff, S. 2003, *A&A*, 400, 1007
- Done, C. & Nayakshin, S. 2001, *MNRAS*, 328, 616
- Dove, J. B., Wilms, J., & Begelman, M. C. 1997a, *ApJ*, 487, 747
- Dove, J. B., Wilms, J., Maisack, M. G., & Begelman, M. C. 1997b, *ApJ*, 487, 759
- Dubus, G., Lasota, J., Hameury, J., & Charles, P. 1999, *MNRAS*, 303, 139
- Falcke, H. 1996, *ApJ*, 464, L67
- Gallo, E., Fender, R. P., & Pooley, G. G. 2003, *MNRAS*, 344, 60
- Georganopoulos, M., Aharonian, F. A., & Kirk, J. G. 2002, *A&A*, 388, L25
- George, I. M. & Fabian, A. C. 1991, *MNRAS*, 249, 352
- Houck, J. C. & Denicola, L. A. 2000, in *ASP Conf. Ser. 216: Astronomical Data Analysis Software and Systems IX*, Vol. 9, 591
- Maccarone, T. J. 2002, *MNRAS*, 336, 1371
- Magdziarz, P. & Zdziarski, A. A. 1995, *MNRAS*, 273, 837
- Malzac, J., Beloborodov, A. M., & Poutanen, J. 2001, *MNRAS*, 326, 417
- Markoff, S., Falcke, H., & Fender, R. 2001, *A&A*, 372, L25
- Markoff, S., Nowak, M., Corbel, S., Fender, R., & Falcke, H. 2003, *A&A*, 397, 645
- McClintock, J. E. & Remillard, R. A. 2003, in *Compact Stellar X-ray Sources*, Eds. W.H.G. Lewin and M. van der Klis, Cambridge University Press, in press (astro-ph/0306213)
- Miller, J. M., Ballantyne, D. R., Fabian, A. C., & Lewin, W. H. G. 2001, *MNRAS*, 555, 477
- Nayakshin, S. & Dove, J. B. 2001, *ApJ*, 560, 885
- Nowak, M. A., Wilms, J., & Dove, J. B. 2002, *MNRAS*, 332, 856
- Pottschmidt, K., Wilms, J., Nowak, M. A., Pooley, G. G., Gleissner, T., Heindl, W. A., Smith, D. M., Remillard, R., & Staubert, R. 2003, *A&A*, 407, 1039
- Pounds, K. A., Nandra, K., Stewart, G. C., George, I. M., & Fabian, A. C. 1990, *Nature*, 344, 132

- Poutanen, J., Krolik, J. H., & Ryde, F. 1997, MNRAS, 221, 21p
- Reynolds, C. S. & Fabian, A. 1997, MNRAS, 290, 1p
- Reynolds, C. S. & Nowak, M. A. 2003, Phys. Rep., 377, 389
- Ross, R. R., Fabian, A. C., & Young, A. 1999, MNRAS, 306, 462
- Shakura, N. I. & Sunyaev, R. A. 1973, A&A, 24, 337
- Stern, B. E., Begelman, M. C., Sikora, M., & Svensson, R. 1995, MNRAS, 272, 291
- Stirling, A. M., Spencer, R. E., de la Force, C. J., Garrett, M. A., Fender, R. P., & Ogley, R. N. 2001, MNRAS, 327, 1273
- Wu, K., Soria, R., Hunstead, R. W., & Johnston, H. M. 2001, MNRAS, 320, 177
- Zdziarski, A. A., Johnson, W. N., Done, C., Smith, D., & McNaron-Brown, K. 1995, ApJ, 438, L63
- Życki, P. T., Done, C., & Smith, D. A. 1997, ApJ, 488, L113+